BIOCHEMISTRY
including biophysical chemistry & molecular biology

ARTICLE

pubs.acs.org/biochemistry

An Arginine Residue Instead of a Conserved Leucine Residue in the Recognition Helix of the Finger 3 of Zif268 Stabilizes the Domain Structure and Mediates DNA Binding

Shigeru Negi,[†,§] Miki Imanishi,[‡,§] Maeko Sasaki,[†] Kazuya Tatsutani,[‡] Shiroh Futaki,[‡] and Yukio Sugiura[*,†]

[†]Faculty of Pharmaceutical Sciences, Doshisha Women's University, Koudo, Kyotanabe-Shi 610-0395, Japan

[‡]Institute for Chemical Research, Kyoto University, Uji 611-0011, Japan

Supporting Information

ABSTRACT: The Cys_2His_2-type zinc finger is a common DNA binding motif that is widely used in the design of artificial zinc finger proteins. In almost all Cys_2His_2-type zinc fingers, position 4 of the α-helical DNA-recognition site is occupied by a Leu residue involved in formation of the minimal hydrophobic core. However, the third zinc finger domain of native Zif268 contains an Arg residue instead of the conserved Leu. Our aim in the present study was to clarify the role of this Arg in the formation of a stable domain structure and in DNA binding by substituting it with a Lys, Leu, or Hgn, which have different terminal side-chain structures. Assessed were the metal binding properties, peptide conformations, and DNA-binding abilities of the mutants. All three mutant finger 3 peptides exhibited conformations and thermal stabilities similar to the wild-type peptide. In DNA-binding assays, the Lys mutant bound to target DNA, though its affinity was lower than that of the wild-type peptide. On the other hand, the Leu and Hgn mutants had no ability to bind DNA, despite the similarity in their secondary structures to the wild-type. Our results demonstrate that, as with the Leu residue, the aliphatic carbon side chain of this Arg residue plays a key role in the formation of a stable zinc finger domain, and its terminal guanidinium group appears to be essential for DNA binding mediated through both electrostatic interaction and hydrogen bonding with DNA phosphate backbone.

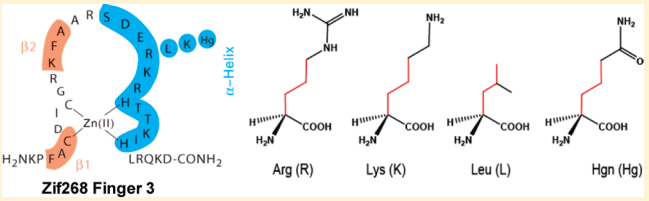

The classical C_2H_2-type zinc finger motif is a common DNA binding motif composed of the highly conserved sequence (Phe/Tyr)-X-Cys-X(2-4)-Cys-X3-(Phe/Tyr)-X5-Leu-X2-His-X(3-5)-His (where X represents any amino acid), which folds into a globular $\beta\beta\alpha$ structure.[1] Within this motif, a Zn(II) is tetrahedrally coordinated by the conserved Cys and His residues. In addition, the conserved hydrophobic residues, which are located in the β-sheet (Phe/Tyr) and α-helix (Leu), form a hydrophobic core that stabilizes the fold of the motif (Figure 1). In an earlier report, we described the relationship between the stability of the hydrophobic core of the GAGA-zinc finger domain and its DNA binding function as well as the importance of the conserved Leu residue for both the stability of the zinc finger structure and DNA binding.[2] However, the contribution made by the various conserved residues in the motif to the structure and function of the zinc finger is still not fully understood. Consequently, although the methodologies used to design zinc finger proteins that bind to desired DNA sequences are now well established,[3−6] it remains difficult to manipulate the zinc finger backbone for the purpose of developing artificial zinc finger proteins. Additional information about the relationships between the structure of the zinc finger backbone and its DNA binding function will be needed before the full potential of these proteins can be realized.

The DNA binding domain of the mouse transcription factor Zif268 contains three C_2H_2-type zinc finger motifs and is one of the best characterized zinc finger domains used in the design of artificial zinc finger proteins.[7−10] Interestingly, the third zinc finger domain of native Zif268 contains an Arg residue instead of the conserved Leu residue (Figure 2A). Analysis to the crystal structure of Zif268 in complex with DNA revealed that this Arg residue (Arg78) makes a water-mediated contact with the DNA phosphate backbone.[8] Therefore, to clarify the contribution made by Arg78 to formation of the hydrophobic core of the domain and to DNA binding, we introduced a series of mutations at that position. The side chain of Arg is a three-carbon aliphatic straight chain with a positively charged terminal guanidinium group able to engage in electrostatic interactions and form hydrogen bonds with the phosphate groups of the DNA backbone. By substituting this Arg residue with three other aliphatic amino acids, Lys, Leu, or Hgn, we examined its function from the standpoint of its hydrophobicity, its role as a hydrogen-bonding donor, and the importance of its positive charge (Figure 2A,B). Hgn is an amino acid that does not occur in nature; it has an aliphatic side chain similar to Lys but differs from Lys in that it has a neutral amide group. In addition, to determine whether the function of the Arg residue in finger 3 (f3) is generally adaptable to C_2H_2 zinc finger motifs or is distinctive of the Zif268

Received: May 6, 2011
Revised: June 19, 2011
Published: June 21, 2011

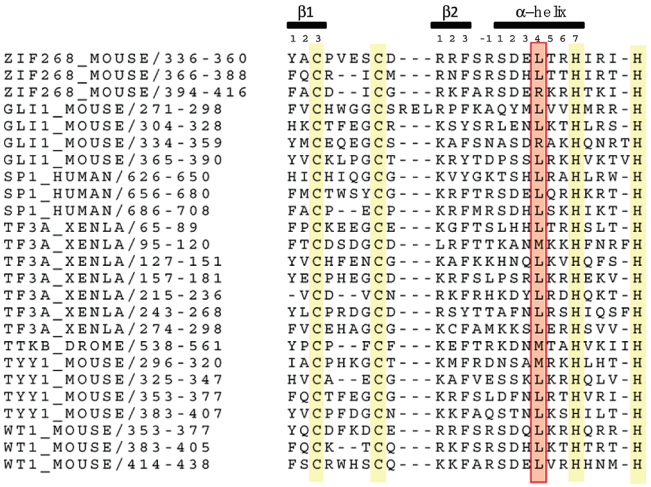

Figure 1. A search of the Pfam database (available on http://pfam.sanger.ac.uk) was used for sequence alignment of the Zif268 zinc finger core with other selected zinc fingers known to have the general structure (Phe/Tyr)-X-Cys-X(2-4)-Cys-X3-(Phe/Tyr)-X5-Leu-X2-His-X(3-5)-His. Zn(II) binding residues (Cys and His) are highlighted in yellow. The locations of the DNA-recognition α-helix and two β-strands are indicated above with the numbering of the positions. The key amino acid in the α-helix is highlighted by red box.

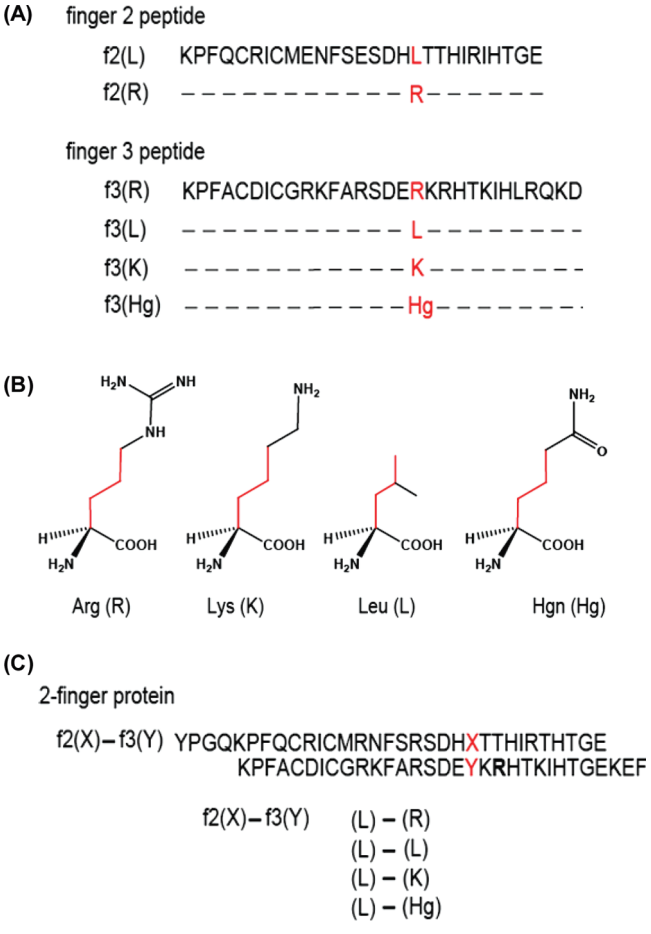

Figure 2. (A) Amino acid sequences of the Zif268 f2 and f3 zinc finger mutant peptides. (B) Structures of the aliphatic amino acids used for the point mutations. (C) Amino acid sequences of the 2-finger Zif268 zinc finger mutants.

f3 (Figure 2A), the conserved Leu residue in finger 2 (f2) of native Zif268 was also substituted with an Arg residue.

MATERIALS AND METHODS

Preparation of f3 Domains. Fmoc-protected amino acids for peptide synthesis (excluding Hgn) were purchased from Peptide Institute, Inc. Fmoc-protected Hgn was synthesized by Watanabe Chemical Industry, Ltd. Synthesis of each individual finger domain was performed on TGS-RAM resin (Shimadzu Corp.) using the solid-phase method with a Shimadzu PSSM-8 synthesizer. The Fmoc chemistry was carried out using a typical protocol with HBTU/HOBT serving as the coupling reagent. After the synthesis, the peptides were removed from the resin by incubation for 2 h with a cocktail consisting of 86% trifluoroacetic acid, 2.5% water, 5% 1,2-ethanedithiol, 5% thioanisole, and 1.5% triethylsilane. The crude peptides were then precipitated in ice-cold ether, separated by centrifugation, washed three times with cold diethyl ether, and finally dissolved in water and lyophilized. The peptide purification was performed using a RP-HPLC system, Model L-7100 (Shimadzu Corp.), employing a COSMOSIL RP-C_{18} column (10 × 250 mm) (Nacalai Tesque, Inc.). Peptides were eluted using a linear acetonitrile−water gradient containing 0.1% trifluoroacetic acid. The fidelity of the products was confirmed by matrix-assisted laser desorption time-of-flight mass spectrometry (MALDI-TOF MASS) using Voyager DE STR (AB SCIEX); M_{calcd}: 3803.4 Da and $[M-H]_{observed}$: 3803.4 Da (Arg, wild-type), M_{calcd}: 3775.4 Da and $[M-H]_{observed}$: 3775.3 Da (Lys mutant), M_{calcd}: 3760.4 Da and $[M-H]_{observed}$: 3760.0 Da (Leu mutant), M_{calcd}: 3789.4 Da and $[M-H]_{observed}$: 3788.3 Da (Hgn mutant). After purification, the peptides were >99% pure as evidenced by the single HPLC peak.

UV Absorption Spectroscopy. UV−vis absorption spectra were recorded on a Beckman Coulter DU7400 diode array spectrophotometer at 20 °C in Tris-HCl buffer (10 mM, pH 7.5) containing NaCl (50 mM) in a capped cell having a 1 cm path length. All the presented spectra were normalized by $\varepsilon = A/lc$, where ε is the extinction coefficient (M^{-1} cm^{-1}), l is the path length of the cell (cm), and c is the peptide concentration (M).

CD Spectroscopy. All the CD experiments were carried out using a JASCO J-720 spectropolarimeter. The spectra were recorded from 195 to 260 nm in the continuous mode with a 1 nm bandwidth, a 1 s response, and a scan speed of 50 nm min^{-1}. Each spectrum represents the average of 20 scans recorded at 20 °C in Tris-HCl buffer (10 mM, pH 8.0) containing NaCl (50 mM) in a capped cell having a 0.1 cm path length under a nitrogen atmosphere. The concentrations of the peptide stock solutions were spectrophotometrically estimated. Variable temperature experiments were performed using 1 °C temperature increments between 5 and 85 °C with an equilibration time of 5 min. Unfolding of the Zif268 peptides was detected by monitoring changes in the CD spectrum.

NMR Spectroscopy. NMR experiments were performed at 20 °C using a Bruker AVANCE500 500 MHz spectrometer. The NMR samples were prepared by dissolving the lyophilized peptide powder in phosphate buffer (20 mM) containing DSS as an internal reference for the ^1H chemical shifts. In all experiments, the peptide concentration was 300 μM, and the pH was adjusted to 7.0 using concentrated NaOH and HCl. Variable temperature experiments were performed in the presence of Zn(II) (1.5 equiv) using 10 °C temperature increments

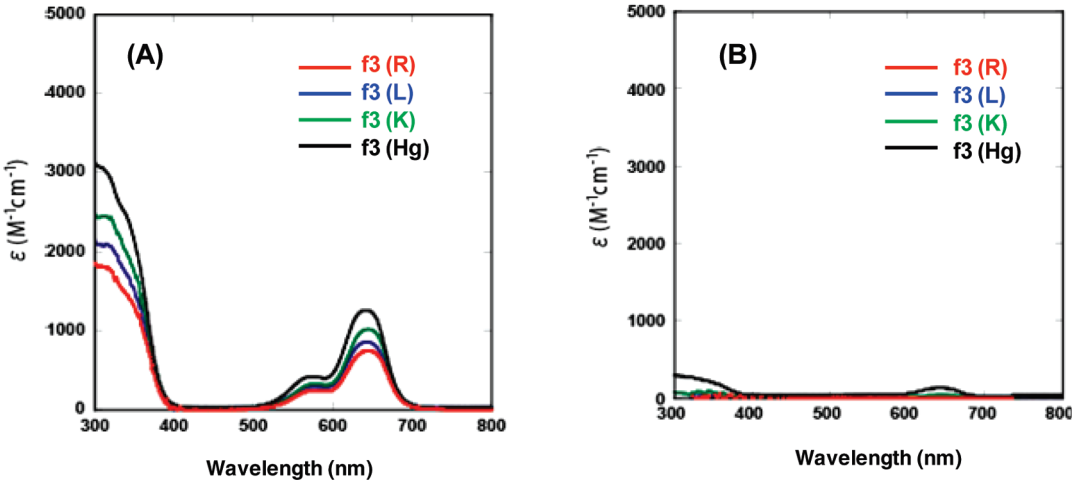

Figure 3. UV−vis absorption spectra of Co(II)−f3 peptide complexes (25 μM) in Tris-HCl (10 mM)/NaCl (50 mM), pH 7.5 (path length 1 cm) in recorded in the absence (A) and presence (B) of an equivalent amount of Zn(II) at 20 °C.

between 20 and 80 °C. The H_2O signal was suppressed using a WATERGATE pulse sequence.[11]

Preparation of 2-Finger Proteins. An expression vector for f2(L)f3(R), pEV-f2(L)f3(R), was created by PCR using pEV-ZF3[12] as a template. The PCR product was cleaved using *Nde*I and *Eco*RI and inserted into pEV-3b, a multicloning-site variant of pET-3b (Novagen). The DNA fragments encoding the 2-finger mutants were amplified by PCR using T7 primers and pEV-f2(L)f3(R) to introduce the point mutations (Figure 2C). The amplified DNA fragments were then cleaved by *Nde*I and *Eco*RI and inserted into pEV-3b, after which the sequences were confirmed using a 3130 genetic analyzer (Applied Bio Systems), and each expression vector was transformed into the *Escherichia coli* strain BL21(DE3) (Novagen). The *E. coli* cells were grown at 37 °C until the OD_{600} = 0.6. They were then incubated for an additional 12 h at 20 °C in the presence of 0.1 mM IPTG and 0.1 mM $ZnCl_2$ to obtain the zinc finger proteins. The over-expressed proteins were purified by cation-exchange chromatography using High S (Bio-Rad Laboratories) and Resource S (GE Healthcare) columns, and the final purification was by gel filtration chromatography on a Superdex 75 column (GE healthcare). The fidelity of the each purified 2-finger protein was confirmed by SDS-PAGE.

Gel Mobility Shift Assays. Each reaction mixture contained 10 mM Tris-HCl (pH 8.0), 50 mM NaCl, 1 mM dithiothreitol, 10 μM $ZnSO_4$, 0.05% Nonidet P-40, 20 ng/μL calf thymus DNA, 40 ng/μL BSA, 5% glycerol, 2.5 nM FITC-end-labeled target DNA fragment, and the serially diluted zinc finger protein. After incubation at 20 °C for 0.5 h, the samples were run on an 8% polyacrylamide gel in 89 mM Tris-borate buffer at room temperature. The bands were visualized using a Fluorimager (Molecular Dynamics) and analyzed using ImageJ. The equilibrium dissociation constant (K_d) of each protein−DNA fragment complex was evaluated by fitting the experimentally obtained values of θ_b (θ_b, the fraction of labeled DNA bound to the protein) to eq 1 using the Kaleida Graph program (Abelbeck software).

$$\theta_b = \{([P] + [D] + K_d) - \sqrt{([P] + [D] + K_d)^2 - 4[P][D]}\}/2[D] \quad (1)$$

RESULTS AND DISCUSSION

Zinc Coordination Chemistry of Zif268 f3 Domains. To determine whether the three constructed f3 single finger mutants, f3(L), f3(K), and f3(Hg), retain the tetrahedral metal coordination geometry seen with the wild-type peptide f3(R), we used UV−vis absorption spectroscopy to study their peptide−metal coordination chemistry. Because Zn(II) has a fully occupied d electron shell (d^{10}), it is spectroscopically silent. Consequently, metal coordination of zinc fingers is often investigated using Co(II) as a spectroscopic probe for the Zn(II) binding site, since the coordination properties of the two ions share some similarity.[13,14] The UV−vis spectra of Co(II) in complex with each of the mutants are compared with that of the wild-type peptide in Figure 3. The UV−vis spectra for all three f3 mutants are similar to that of the wild-type peptide. The intense absorption bands in the near-UV regions around 316 and 340 nm are indicative of the Cys-S^-→ Co(II) ligand-to-metal charge transfer (LMCT) transition.[15] The magnitude of the extinction coefficient (ε) at 320 nm reflects the number of thiol-containing ligands coordinated to the metal and averages about 900−1200 M^{-1} cm^{-1} per Cys-S^-−Co(II) bond.[16,17] We found the ε values at 320 nm to be around 2000 M^{-1} cm^{-1} for all the peptides, which suggests the peptides use two thiol groups for coordination of the Co(II).

The coordination geometry of the Co(II) within the peptide−metal complex can be estimated on the basis of the ligand-field theory; the optical transitions of a tetrahedral Co(II) species exhibit an intense d−d absorption band in the 625 ± 50 nm region due to the small ligand-field stabilization energy.[18] All of the f3 peptides showed similar d−d transition bands at around 650 nm, indicating that Co(II) has a tetrahedral coordination geometry (Figure 3A). In competition experiments, the d−d transition band (~650 nm) observed with the Co(II)−peptide complexes disappeared upon addition of an equivalent amount of the spectroscopically inactive Zn(II) (Figure 3B). This implies that Zn(II) displaces the Co(II) and occupies the metal binding site of the peptides due to the difference in the ligand-field stabilization energy between Co(II) and Zn(II).[19] Thus, the UV−vis data clearly show that replacing the Arg at position 4 of the α-helix region in f3 with any of the three aliphatic amino acids

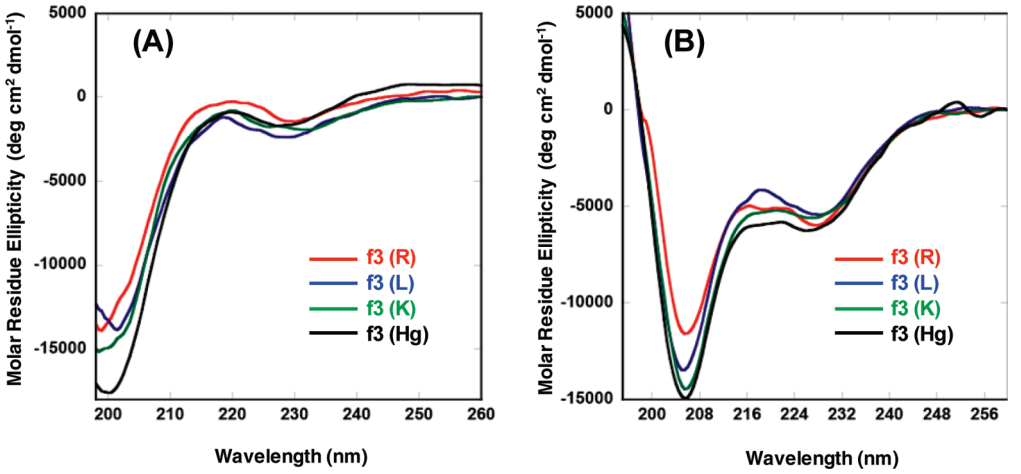

Figure 4. CD spectra for f3 peptides (25 μM) in Tris-HCl (10 mM)/NaCl (50 mM), pH 7.5 (path length 0.1 cm), recorded in the absence (A) and presence (B) of 1.5 equiv of Zn(II) at 20 °C.

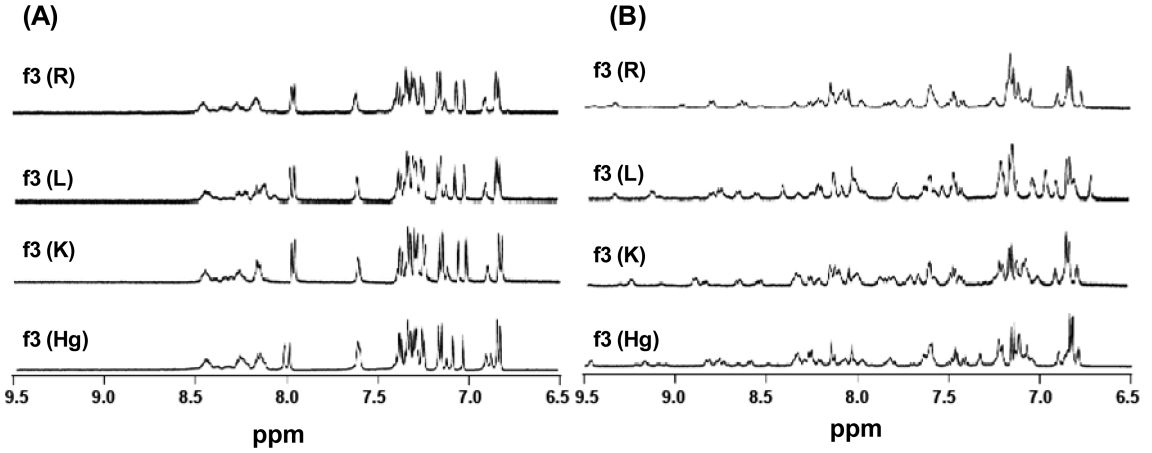

Figure 5. ^{1}H NMR spectra for f3 peptides (300 μM) in 90% H_2O/10% D_2O with 20 mM phosphate buffer, pH 7.0, recorded in the absence (A) and presence (B) of 1.5 equiv of Zn(II) at 20 °C.

tested (Lys, Leu, and Hgn) does not alter the coordination geometry of the Zn(II) binding; i.e., the zinc finger state is similar in all four f3 peptides.

Folded Structures of the Zif268 f3Mutants. CD spectroscopy is a powerful tool for determining the secondary structure of peptides in solution,[20] and the CD signature of the zinc finger domain has been well documented.[14,21−24] Sénèque et al. recently reported that the changes in the CD signal of zinc finger upon Zn(II) binding reflect both the change in the structure of peptide and the appearance of LMCT bands.[24] We therefore used this technique to compare the conformational properties of the f3 mutants with those of wild-type f3(R). Figure 4 shows the CD spectra for the four peptides at 20 °C. In the absence of Zn(II), all of the peptides display a negative band near 200 nm ($\pi \rightarrow \pi^*$ electronic transition) and a small shoulder around 222 nm (n $\rightarrow \pi^*$ electronic transition), which suggests the peptides are in a largely random coil conformation (Figure 4A). Upon addition of Zn(II), dramatic changes in the CD spectrum were observed for all of the peptides. There was a significant increase in the α-helix negative molar ellipticity signature around 222 nm as well as a marked decrease in the random coil negative molar ellipticity signature near 200 nm. This suggests all of the peptides fold into the characteristic zinc finger $\beta\beta\alpha$ structure and that the helix content is comparable among the four peptides (Figure 4B). The slight differences observed in the CD spectra could be due to minor alterations in the structures of the zinc finger domain caused by the mutations. As judged from both the UV−vis and CD results, all of the f3 mutants have similar zinc coordination geometries and nearly the same secondary structures, despite the different aliphatic side chains at position 4 of the α-helix region.

We next investigated the microenvironmental changes in the mutant f3 domains by using the ^{1}H NMR technique to estimate the structural changes of f3 domains caused by the Arg substitutions. NMR spectroscopy is a promising method for detecting both the secondary and tertiary structures of folded proteins, as proton chemical shifts are highly sensitive indicators of a peptide's structural integrity. The proton NMR spectra of the f3 peptides recorded at 20 °C in aqueous buffer in the absence and presence of Zn(II) are shown in Figure 5. The signal for the amide protons is seen, as expected, in the chemical shift around 8.0 ppm. In the absence of Zn(II), the NMR spectra for all four f3 peptides exhibited the spectral characteristics of unfolded

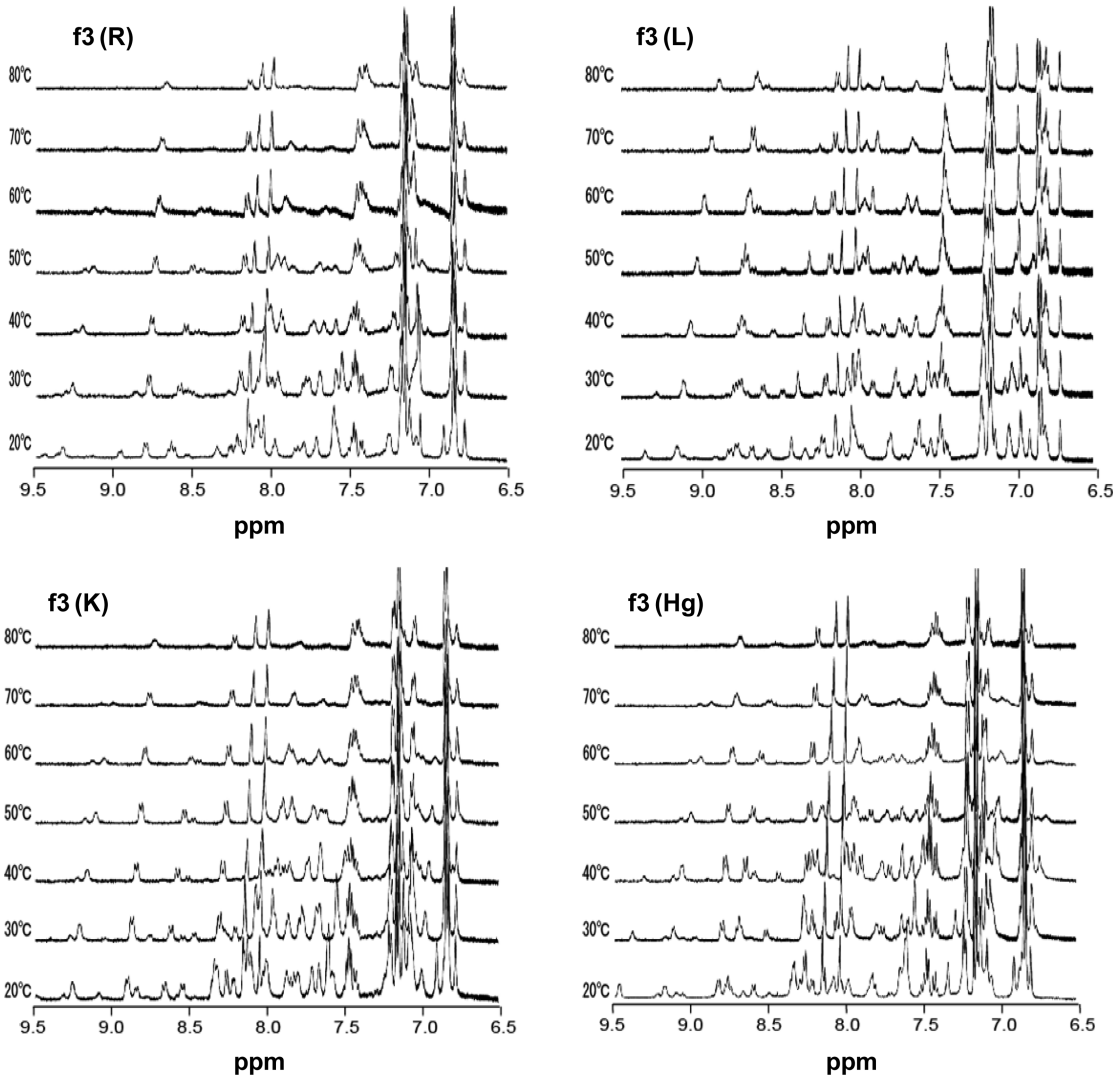

Figure 6. Temperature-dependent ^{1}H NMR spectra for f3 peptides recorded in the presence of 1.5 equiv of Zn(II) in 90% H_2O/10% D_2O with 20 mM phosphate buffer, pH 7.0, at temperatures between 20 and 80 °C.

structures, including less dispersion in the downfield amide proton region (Figure 5A). In the presence of Zn(II), by contrast, the NMR spectra of these peptides provided strong evidence of typically folded structures. In fact, clearly resolved and dispersed amide signals were observed in the downfield amide proton region (Figure 5B, from 7.5 to 9.5 ppm). The slight differences in the NMR spectra of these peptides could be due to minor structural differences caused by the substitution of Arg. These NMR results provide qualitative evidence that all of the mutated f3 peptides fold into a conformation similar to the wild-type f3 at 20 °C, which is consistent with the CD data.

Thermal Stability of Zif268 f3Mutants. To estimate how subtle changes in the amino acid side chain affect the thermal stability of the f3 peptides, we carried out a set of variable temperature CD (VT-CD) and NMR (VT-NMR) experiments. The VT-CD results are shown in Figure S1. All of the peptides, including the wild-type peptide, exhibited only slight spectral changes at temperatures ranging from 15 to 85 °C, and no global changes in the domain structures of the mutant f3 peptides were observed. That is, the wild-type and mutants have similar thermal stabilities, and no significant changes in the secondary structures of the mutant f3 peptides were induced by substituting the Arg with other aliphatic amino acids. These CD spectral changes are consistent with our earlier results showing similar cooperative folding for wild-type and mutant GAGA zinc finger domains.[2,21]

VT-NMR experiments can provide additional information about both the precise conformational equilibrium and thermal stability of the f3 domains in aqueous solution. In our earlier work, VT-NMR experiments revealed clear differences in the intrinsic stability of mutant GAGA peptides that were dependent on the aliphatic amino acid residues involved in the formation of the hydrophobic core; nonetheless, these peptides showed nearly identical secondary structures and thermal stabilities in CD experiments.[2] This suggests CD spectroscopy is not sufficient for detecting slight structural changes at the residue level caused by mutations within the zinc finger domains; instead, CD spectra provide information on the overall conformation of peptides and proteins in aqueous solution. Figure 6 shows the VT-NMR spectra for the wild-type and mutant f3 peptides. In all cases, the NMR spectra showed good overall dispersion in the amide region at low temperatures, reflecting the stable structure, and then a broadening of the upfield chemical shift and loss of signal

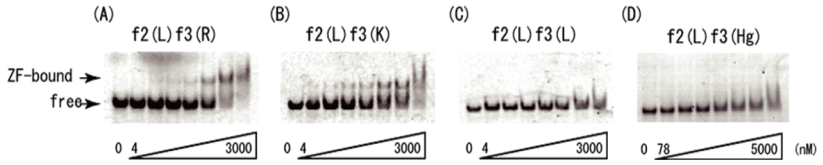

Figure 7. Gel mobility shift assays assessing the binding of the indicated zinc finger peptides to a target DNA sequence. Peptide concentrations: 0, 4, 12, 37, 111, 333, 1000, and 3000 nM (A−C) and 78, 156, 313, 625, 1250, 2500, and 5000 nM (D).

Table 1. K_d Values for the Binding of 2-Finger Proteins (f2−f3) of Zif268 Zinc Finger Domain and the Mutant Proteins at the Fourth Position of the Helix of the Finger 2 or 3 to the Target DNA

		K_d (μM) of 2-finger proteins[a]
wild type	f2(L)f3(R)	0.67 ± 0.11
f3 mutants	f2(L)f3(K)	2.1 ± 0.4
	f2(L)f3(L)	N.B.[b]
	f2(L)f3(Hg)	N.B.
f2 mutants	f2(R)f3(R)	0.60 ± 0.17

[a] The K_d values were determined by gel mobility shift assays. All values reported are the mean of at least three measurements (mean ± s.d.). [b] N.B.: no binding.

intensity with increasing temperature (especially in the range of 8.5−9.5 ppm). No evidence of any precipitation was detected at the higher temperature. These data suggest that, for all of the peptides, as the temperature was increased, the time scale of the motion of the backbone structures approaches that of the NMR and that there are no differences in the structural stability between the wild-type and mutant peptides.

Both the VT-CD and VT-NMR experiments clearly show that the stability of the zinc finger domain structure (hydrophobic core structure) was unaffected by substitution of the Arg at position 4 of the helix region with any of the aliphatic amino acids tested. This indicates that the common three-carbon aliphatic straight chain structure of these amino acids (red parts in Figure 2B) plays a crucial role in the formation of a stable folded structure and that the fold is not dependent on the terminal functional group of side chain.

DNA Binding of the Zif268 Zinc Finger Mutants. The abilities of the mutant f3 peptides to bind DNA were examined using gel mobility shift assays. Any significant differences in the DNA-binding properties of the wild-type and mutant peptides would be particularly noteworthy, since all three mutant peptides possess domain structures and stabilities that are similar to the wild-type peptide. We used two-finger peptides consisting of f2 and f3 of the Zif268 DNA binding domain to evaluate the effects of the mutations on binding; the DNA binding affinity of a single finger peptide was too weak to evaluate the effects of mutation (Figure 2C). With the exception of the Hgn mutant, which was chemically synthesized, all of the 2-finger peptides were purified from an *E. coli* expression system. As the target DNA, we used dsDNA containing the Zif268 binding site (5′-GCG TGG gcg-3′; the capital letters correspond to the 2-finger binding site). The results are shown in Figure 7 and Table 1. The wild-type peptide, f2(L)f3(R), in which position 4 of the α-helix is a Leu in f2 and an Arg in f3, bound the DNA with a K_d of 0.67 μM. The f3 Lys mutant f2(L)f3(K) also showed a band shift, but its DNA-binding affinity was lower than that of the wild-type peptide. Taking into consideration that the structure and stability of the f3 Lys mutant is comparable to the wild-type peptide, this result suggests that the guanidinium group of Arg has a greater potential to interact with the DNA than the amino group of Lys. On the other hand, the f3 Leu mutant showed no band shifts, even at a concentrations of 3 μM. This suggests that hydrogen-bonding donors and/or positively charged side chains at position 4 of the f3 α-helix are required for DNA binding, even though the zinc binding and peptide folding properties are indistinguishable among these peptides.

To assess the contribution made by positively charged side chains to DNA binding, we also examined the DNA binding ability of the f2(L)f3(Hg) peptide. As mentioned earlier, the side chain of Hgn consists of an aliphatic carbon chain the same length as the Lys side chain and a terminal amide group that is capable of forming a hydrogen bond but differing from the terminal amino group of Lys in that it is neutrally charged. In the case of f2(L)f3(Hg) peptide, no shift band was observed to the target DNA at concentrations under 5 μM. Given that chemically synthesized f2(L)f2(K) peptide had a DNA binding affinity comparable to the *E. coli*.-expressed f2(L)f2(K) peptide (data not shown), the result obtained with the f2(L)f3(Hg) peptide cannot be attributed to the method of its synthesis. Considering the differences between the side chains of Hgn and Lys, the result strongly suggests that a positively charged side chain contributes significantly to the DNA binding. In addition to the formation of hydrogen bonds with the DNA phosphate backbone via a water molecule, as previously suggested by X-ray crystal structural analysis of a DNA-Zif268 complex,[8] electrostatic interaction between the positively charged side chain of the Arg residue and the negatively charged DNA phosphate backbone may be required to achieve the proper distance between the hydrogen donor and acceptor needed to form the water-mediated hydrogen bond.

Finally, gel mobility shift assays of the f2 mutant f2(R)f3(R) were performed in order to determine whether the conserved Leu residue at position 4 of the α-helix of f2 can be substituted by Arg and whether the introduced Arg can contribute to the DNA binding of f2. Table 1 shows the K_d of the f2 mutant for the target DNA. The f2(R)f3(R) peptide bound the DNA with a K_d of 0.60 μM, which is comparable to the wild-type peptide, f2(L)f3(R). This indicates that the Arg residue can substitute for Leu but that the guanidinium group of the Arg side chain in f2 does not actively contribute to the DNA binding. In addition, the fact that f2(R)f3(R) and f2(L)f3(R) have comparable affinities for DNA is consistent with the idea that the aliphatic carbon chain of Arg contributes to the proper formation of the hydrophobic core of f2, as it does in f3.

In summary, we focused on the third zinc finger domain of Zif268, which contains an Arg residue instead of the conserved Leu residue found in most zinc finger proteins. To clarify the

contribution made by this Arg residue to zinc finger domain structure and DNA binding, we investigated the effects of substituting the Arg with Lys, Leu, or Hgn. The aliphatic carbon chain of the Arg residue contributes to the proper formation of the hydrophobic core of the zinc finger domain, while the Arg guanidinium group in f3 contributes to strong DNA binding mediated by electrostatic interaction and hydrogen bonding with the DNA phosphate backbone. Our findings on the function of the Arg residue in the third zinc finger domain of Zif268 may also be useful for the design of novel artificial zinc finger proteins.

■ ASSOCIATED CONTENT

Supporting Information. CD spectra of peptides in the presence of $ZnCl_2$ at different temperatures (Figure S1). This material is available free of charge via the Internet at http://pubs.acs.org.

■ AUTHOR INFORMATION

Corresponding Author

*Tel: +81-774-8649. Fax: +81-774-8652. E-mail: ysugiura@dwc.doshisha.ac.jp.

Author Contributions

§These authors contributed equally to this work.

Funding Sources

This work was supported in part by grants from the Ministry of Education, Culture, Sports, Science, and Technology, Japan; Hayashi Memorial Foundation for Female Natural Scientists; and the Kurata Memorial Hitachi Science and Technology Foundation.

■ ACKNOWLEDGMENT

We thank D. J. Segal for helpful discussions. This work was supported in part by grants from the Ministry of Education, Culture, Sports, Science, and Technology, Japan; Hayashi Memorial Foundation for Female Natural Scientists; and the Kurata Memorial Hitachi Science and Technology Foundation.

■ ABBREVIATIONS

CD, circular dichroism; DSS, 2,2-dimethyl-2-silapentane-5-sulfonate sodium salt; FITC, fluorescein isothiocyanate; Fmoc, 9-fluorenylmethyloxycarbonyl; HBTU, 2-(1-*H*-benzotriazole-1-yl)-1,1,3,3,-tetramethyluronium hexafluorophosphate; Hgn, Homoglutamine; HOBt, 1-hydroxybenzotriazole; RP-HPLC, reversed-phase high-performance liquid chromatography; Tris, tris(hydroxymethyl)-aminomethane; UV−vis, ultraviolet−visible.

■ REFERENCES

(1) Klug, A. (2010) The discovery of zinc finger and their applications in gene regulation and genome manipulation. *Annu. Rev. Biochem. 79*, 213–231.

(2) Dhanasekaran, M., Negi, S., Imanishi, M., and Sugiura, Y. (2008) Effects of bulkiness and hydrophobicity of an aliphatic amino acid in the recognition helix of the GAGA zinc finger on the stability of the hydrophobic core and DNA binding affinity. *Biochemistry 47*, 11717–11724.

(3) Rebar, E. J., and Pabo, C. O. (1994) Zinc finger phage: affinity selection of fingers with new DNA-binding specificities. *Science 263*, 671–673.

(4) Rebar, E. J., Greisman, H. A., and Pabo, C. O. (1996) Phage display methods for selecting zinc finger proteins with novel DNA-binding specificities. *Methods Enzymol. 267*, 129–149.

(5) Segal, D. J., Dreier, B., Beerli, R. R., and Barbas, C. F., III (1999) Toward controlling gene expression at will: selection and design of zinc finger domains recognizing each of the 5′-GNN-3′ DNA target sequences. *Proc. Natl. Acad. Sci. U.S.A. 96*, 2758–2763.

(6) Klug, A. (1999) Zinc finger peptides for the regulation of gene expression. *J. Mol. Biol. 293*, 215–218.

(7) Pavletich, N. P., and Pabo, C. O. (1991) Zinc finger-DNA recognition: crystal structure of a Zif268-DNA complex at 2.1 Å. *Science 252*, 809–817.

(8) Elrod-Erikson, M., Rould, M. A., Nekludova, L., and Pabo, C. O. (1996) Zif268 protein-DNA complex refined at 1.6 Å: a model system for understanding zinc finger-DNA interactions. *Structure 4*, 1171–1180.

(9) Wolfe, S. A., Grant, R. A., and Pabo, C. O. (2003) Structure of a designed dimeric zinc finger protein bound to DNA. *Biochemistry 42*, 13401–13409.

(10) Imanishi, M., Nakaya, T., Morisaki, T., Noshiro, D., Fukatki, S., and Sugiura, Y. (2010) Metal-stimulated regulation of transcription by an artificial zinc-finger protein. *ChemBioChem 11*, 1653–1655.

(11) Piotto, M., Saudek, V., and Sklenár, V. (1992) Gradient-tailored excitation for single-quantum NMR spectroscopy of aqueous solution. *J. Biomol. NMR 2*, 661–665.

(12) Morisaki, T., Imanishi, M., Futaki, S., and Sugiura, Y. (2008) Rapid transcriptional activity in vitro and slow DNA binding in vitro by artificial multi-zinc finger protein. *Biochemistry 47*, 10171–10177.

(13) Frankel, A. D., Berg, J. M., and Pabo, C. O. (1987) Metal-dependent folding of a single zinc finger from transcriptional IIIA. *Proc. Natl. Acad. Sci. U.S.A. 84*, 4841–4845.

(14) Nomura, A., and Sugiura, Y. (2002) Contribution of individual zinc ligands to metal binding and peptide folding of zinc finger peptides. *Inorg. Chem. 41*, 3693–3698.

(15) Giedroc, D. P., Keating, K. M., Williams, K. R., Konigsberg, W. H., and Coleman, J. E. (1986) Gene32 protein, the single-stranded DNA binding protein form bacteriophage T4, is a zinc metalloprotein. *Proc. Natl. Acad. Sci. U.S.A. 83*, 8452–8456.

(16) May, S. W., and Kuo, J.-Y. (1978) Preparation and properties of cobalt(II) rubredoxin. *Biochemistry 17*, 3333–3338.

(17) Vašák, M., Kägi, J. H. R., Holmquist, B., and Vallee, B. L. (1981) Spectral studies of cobalt(II)- and Ni(II)-metallothionein. *Biochemistry 20*, 2259–6664.

(18) Bertini, I., and Luchinat, C. (1984) High Spin cobalt(II) as a probe for the investigation of metalloprotein. *Adv. Inorg. Biochem. 6*, 71–111.

(19) Berg, J. M., and Merkle, D. L. (1989) On the metal ion specificity of "zinc finger" proteins. *J. Am. Chem. Soc. 111*, 3759–3761.

(20) Woody, R. W. (1995) Circular dichroism. *Methods Enzymol. 246*, 34–71.

(21) Dhanasekaran, M., Negi, S., Imanishi, M., and Sugiura, Y. (2007) DNA-binding ability of GAGA zinc finger depends on the nature od amino acids present in the β-hairpin. *Biochemistry 46*, 7506–7513.

(22) Struthers, M. D., Cheng, R. P., and Imperiali, B. (1996) Economy in protein design: evolution of a metal-independent $\beta\beta\alpha$ motif based on the zinc finger domains. *J. Am. Chem. Soc. 118*, 3037–3081.

(23) Dahiyat, B. I., and Mayo, S. L. (1997) De novo protein design: fully automated sequence selection. *Science 278*, 82–87.

(24) Sénèque, O., and Latour, J. M. (2010) Coordination properties of zinc finger peptides revisited: ligand competition studied reveal higher affinity for zinc and cobalt. *J. Am. Chem. Soc. 132*, 17760–17774.